

## Measurement of 3D Spreader Position Information using the CCD Cameras and a Laser Distance Measuring Unit

Jung-Jae Lee\* · Gi-Gun Nam\*\* · Bong-Ki Lee\*\*\* · Jang-Myung Lee\*\*\*\*

\*, \*\* Department of Electronics Engineering, Pusan National University, Busan 609-735, Korea

\*\*\* Graduate School, Pusan National University, Busan 609-735, Korea

\*\*\*\* Department of Electronics Engineering, Pusan National University, Busan 609-735, Korea

**Abstract :** This paper introduces a novel approach that can provide the three dimensional information about the movement of a spreader by using two CCD cameras and a laser distance measuring unit in order to derive ALS (Automatic Landing System) in the crane used at a harbor. So far a kind of 2D Laser scanner sensor or laser distance measuring units are used as corner detectors for the geometrical matching between the spreader and a container. Such systems provide only two dimensional information which is not enough for an accurate and fast ALS. In addition to this deficiency in performance, the price of the system is too high to adapt to the ALS. Therefore, to overcome these defects, we proposed a novel method to acquire the three dimensional spreader information using two CCD cameras and a laser distance measuring unit. To show the efficiency of proposed method, real experiments are performed to show the improvement of accuracy in distance measurement by fusing the sensory information of the CCD cameras and a laser distance measuring unit.

**Key words :** Yard crane, Spreader, Skew, Sway, Laser Distance sensor, CCD camera, ATC

### 1. Introduction

Recently, international trade has been increased continuously. Especially export and import container cargos have been increased through the sea. However most of the port systems are manually operated up to now, which limits the flow of cargos. The only automated part of the port is the cargo database. So labor cost increases every year due increasing freight management cost. Also, there is always the danger of casualties.

At the present time, the unmanned automatic control systems for container ports have been investigated around the world (Choi et al., 2002 ; I. Murata, 1993 ; Gutierrez, 1998). Amsterdam port system is completely automated including the loading, transporting and carrying.

The points that have been researched about the port system are AGVs' (Liu 2002), automatic gate systems, loading device systems as well as others. This research focuses on the loading device system which is a typical electro-mechanical system and is the most difficult part for building the automated container terminal.

Our major goal is to obtain accurate spreader position information in order to pick up containers with ALS (Automatic Landing System) as a part of an automated port

system. For implementing the ALS, several methods using the corner detectors with several laser distance sensors have been developed (Korea Institute of machinery, 2001). In this research, a novel approach to measure the distance between the spreader and the container has been proposed by using two CCD cameras and a laser distance measuring unit, which guarantees better economic efficiency and performance than the conventional ones. It has been known that when the cameras are utilized to measure the distance at the outdoors, there are several problems such as susceptibility to dust, illumination and physical shocks. However, these drawbacks are overcome by miniaturizing cameras and developing high performance image processing systems. Actually in Hongkong, small and durable cameras have been used for detecting the matching status between the spreader and the container.

In this research, two CCD cameras and a laser distance measuring unit have been utilized for the measuring the 3D spreader position information. The image data have been pre-processed by the image reduction, edge detection and Hough transformation. With this image processing, the method for calculating the height, the skew angle and the three dimensional movement information, such as sway angle and angular velocity between the spreader and the

\* Corresponding Author : Jung-Jae Lee, swear21@pusan.ac.kr, 051)510-1696

\*\* ggnam@pusan.ac.kr, 051)510-1696

\*\*\* ybkybk2000@pusan.ac.kr, 051)510-1696

\*\*\*\* Jang-Myung Lee, jmlee@pusan.ac.kr, 051)510-2378

container, has been proposed in this paper.

## 2. The crane

Fig. 1 shows a yard crane used in our research, which has 3D (three dimensional) motion capability. The x-axis represents the direction of crane movement on the yard. The y-axis and z-axis represent horizontal movement of the trolley and vertical movement of the spreader, respectively. The height can be defined as the distance between the spreader and the container.

Two CCD cameras are located at the diagonal corners of the spreader so that the images of the container corners can easily be captured. The laser distance sensor is placed in the center of spreader as shown in Fig. 2.

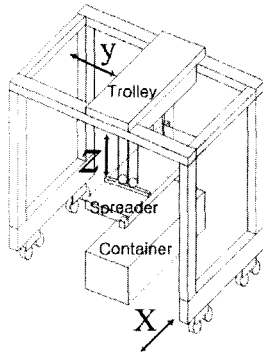


Fig. 1 Overview of a yard crane

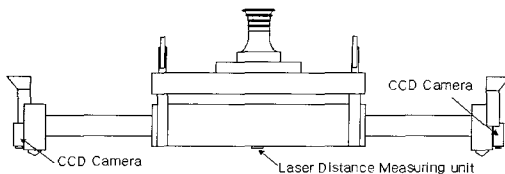


Fig. 2 Front-view of a spreader

## 3. Image processing for detecting container corner

### 3.1 Edge detection

An edge is detected at the locations where the intensity of image changes from a low to a high value or vice versa. In other words, when there is a differential intensity, it is considered as an edge. In general, a partial derivative is used to detect an edge. Fig. 3 shows the edge forms resulted by a first order derivative and a second order derivative at the intensity gradient graph.

The value of the first order derivative represents the existence of an edge and a sign value of the second order derivative indicates a region that has both a high intensity

and low intensity (Sonka, 1993 ; Rafael, 1993).

However, it is difficult to calculate the derivative for each pixel since it takes too much time to be implemented in real time. To save the processing time, a homogeneity operator such as the Sobel mask is used to obtain the edge information, which is illustrated in Fig. 4.  $G_x$  is a horizontal derivative mask and  $G_y$  is a vertical derivative mask.

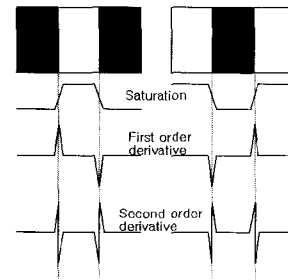


Fig. 3 Edge detection by partial derivative

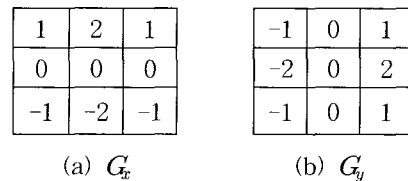


Fig. 4 Sobel mask

### 3.2 Hough transformation for line detection

Hough transformation is a technique which can be used to isolate features of a particular shape within an image (R. O., 1972). To detect lines, Eq. (1) is transformed into polar coordinates, Eq. (2). After extracting the parameters,  $\rho$  and  $\theta$ , the inverse transformation can be carried out to obtain a line equation in the Cartesian coordinates.

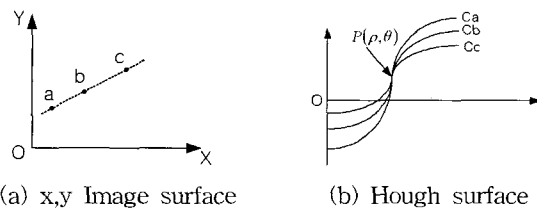


Fig. 5 Line in the Cartesian coordinates and in the polar coordinates

$$y = \alpha x + \beta \tag{1}$$

$$\rho = x \cos \theta + y \sin \theta \tag{2}$$

where  $\alpha = -\frac{\cos \theta}{\sin \theta}$ ,  $\beta = \frac{\rho}{\sin \theta}$ .

Note that the points a, b, and c in x-y coordinates correspond to curves in polar coordinates, respectively; a line corresponds to a point. Therefore the line can be found by using the fact that all the points on a line in an image frame can be represented by a point in polar coordinates. When a point,  $\rho$  and  $\theta$ , is obtained in the polar coordinates,  $x$  values in the Cartesian coordinates can be obtained as,

$$x = \frac{\rho - \beta \sin \theta}{\cos \theta - \alpha \sin \theta} \quad (3)$$

where  $\alpha$  and  $\beta$  are previously defined in Eq. (1).

#### 4. 3D distance information between the container and the spreader

In order for the spreader to grasp the container, the corners of the spreader must match up to the corners of the container. For the purpose, the corners of the spreader are found in the image by using the CCD cameras which are installed diagonally opposite to the corners of spreader, and capture the two corners of the container by image processing. The distance between the spreader and the container is obtained through the geometrical analysis of the corner image information.

##### 4.1 Extracting Image coordinates with the laser distance measuring unit

A pin-hole camera model is used to estimate the real position of the corners in the image frame. The pin-hole camera model provides the relationship between the number of pixels from the center in the image frame and the real distance from the focal axis as it is shown in Fig. 6 (David, 1986 ; Choi et al., 2003 ; Park et al., 2003). Therefore, the relation between the real coordinates (Fig. 6) and the image coordinates (Fig. 7) from the pin-hole camera model can be derived based on the perspective model. The horizontal image angle of the CCD camera on the spreader is represented as  $\theta_x$  and its vertical image angle is represented as  $\theta_y$  in Fig. 6.  $P_{SLCC}$  is the center point of left CCD camera lens and  $P_{SRCC}$  is the center point of right CCD Camera lens in the real coordinates. In Fig. 7, the center point of CCD camera lens is equal to image center point in real coordinates. As the result, the center points of CCD camera lens like  $P_{ILCC}$ ,  $P_{IRCC}$  in image coordinate are not changed when the height between the spreader and the container is changed. In Fig. 6, upper two lines show the real size of an object corresponding to the

CCD camera image when the distance between the spreader and the container is short. If the distance to the real object is not known, for example, as it shown in Fig. 6 as lower two lines, the real object size can be estimated differently for the same image size. Fig. 7 shows that the size of image changes for the same object when the distance to the object is different. When an object is located at long distance, it looks like smaller one than the object at short distance in the image frame. So the distances in the real coordinate from the left corner point of spreader,  $P_{SLS}$ , to the center point of CCD camera lens,  $P_{SLCC}$  is same on the upper plane and on the lower plane in Fig. 6. However the distance between the center point of CCD camera lens,  $P_{ILCC}$ , to the left corner point of spreader,  $P_{ILS1}$ , on the upper plane and the distance between the center point of CCD camera lens,  $P_{ILCC}$ , to the corner point of spreader left,  $P_{ILS2}$ , on the lower plane in Fig. 7 are different in the image coordinates. Note that  $d_x$  is the number of horizontal pixels and  $d_y$  is the number of vertical pixels.

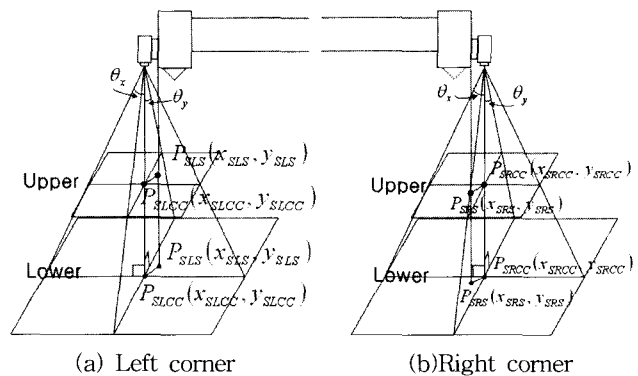


Fig. 6 Spreader corner points in the real coordinates

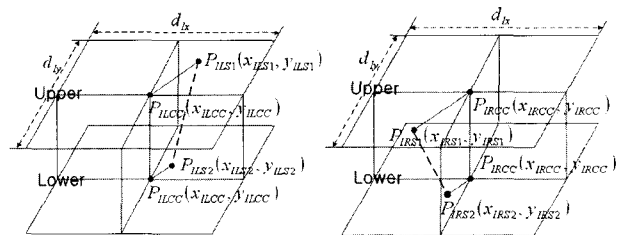


Fig. 7 Image of different height between the spreader and the container

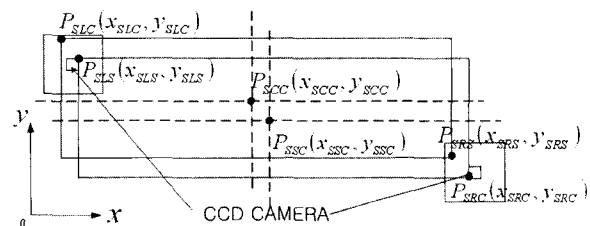


Fig. 8 Container corners and spreader corners

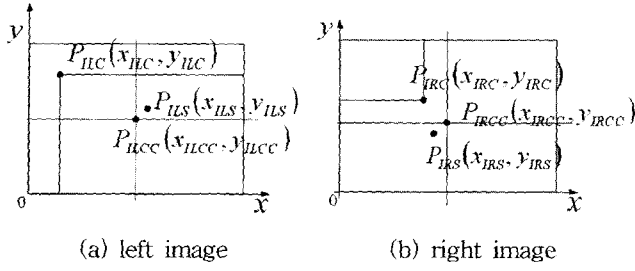


Fig. 9 CCD Camera image data

By comparing Fig. 6 and Fig. 7, it can be recognized that the corner point coordinates of the spreader,  $P_{SLS}$ , are proportional to the height between the container and the spreader.

The image features for the container corners are located opposite to one the other since the CCD cameras are located oppositely as it is shown in Fig. 8. In this figure, the points,  $P_{SLS}$  and  $P_{SRS}$ , are the left and the right corner points of spreader in the real coordinates, while the points,  $P_{SLC}$  and  $P_{SRC}$ , are the left and the right corner points of container in the real coordinates. The point,  $P_{SSC}$ , is the center of spreader and the point,  $P_{SCC}$ , is the center of container in the real coordinates.

In Fig. 9, the points,  $P_{ILS}$  and  $P_{IRS}$ , are the left and the corner points of right spreader in the image coordinates, while the points,  $P_{ILC}$  and  $P_{IRC}$ , are the left and the right corner points of container in the image coordinates.

If the height between the spreader and the container is known then the corner-point coordinates of the spreader in the image frame can be obtained as

$$\begin{pmatrix} x_{ILS} \\ y_{ILS} \\ x_{IRS} \\ y_{IRS} \end{pmatrix} = \frac{1}{2d_{sc}} \begin{pmatrix} x_{SLS} - x_{SLCC} & 0 \\ 0 & y_{SLS} - y_{SLCC} \\ x_{SRS} - y_{SRCC} & 0 \\ 0 & y_{SRS} - y_{SRCC} \end{pmatrix} \begin{pmatrix} \frac{d_{lx}}{\tan \theta_x} \\ \frac{d_{ly}}{\tan \theta_y} \end{pmatrix} + \begin{pmatrix} x_{ILCC} \\ y_{ILCC} \\ x_{IRCC} \\ y_{IRCC} \end{pmatrix} \quad (4)$$

where,  $\theta_x$  is horizontal image angle and  $\theta_y$  is vertical image angle of CCD camera defined in Fig. 6.

#### 4.2 Measuring the height without the laser distance measuring unit

When the laser distance sensor is not available, the height between the container and the spreader can be derived by using the images of the CCD cameras. From the Eq. (4), the height between the container and the spreader can be obtained if we have the coordinates of the corner-points for the spreader. That is, the relationship between the container and the spreader is necessary for

measuring the height. In this paper, we derive corners of the spreader from the image coordinates based on the fact that the corners of the spreader and the container are exactly matched when the spreader holds the container. In other words, if the corners of spreader are exactly matched up with the corners of container then the distance error disappears at the moment.

The symmetrical images are utilized for obtaining the corner coordinates and the sizes of the spreader and container. Since the two CCD cameras are installed diagonally, that is, oppositely to each other *w.r.t* the center of the spreader, the coordinates of the spreader corners are diagonally opposite in the image plane. When the skew angle is zero, the x-coordinate values at the left corner of the spreader and the height can be calculated as follows:

$$x_{ILS} \approx x_{ILC} + (d_{lx} - x_{IRC})/2 \quad (5)$$

$$d_{sc} = \frac{(x_{SLS} - x_{SLCC})d_{lx}}{2(x_{ILS} - x_{ILCC})\tan \theta_x} \quad (6)$$

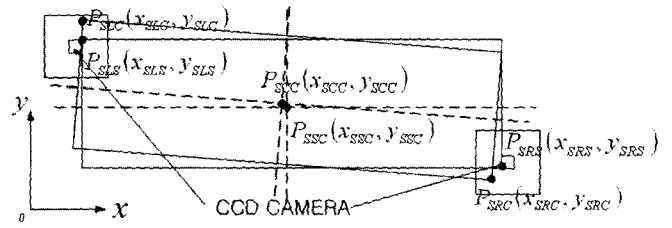


Fig. 10 Container corners and spreader corners with skew angle

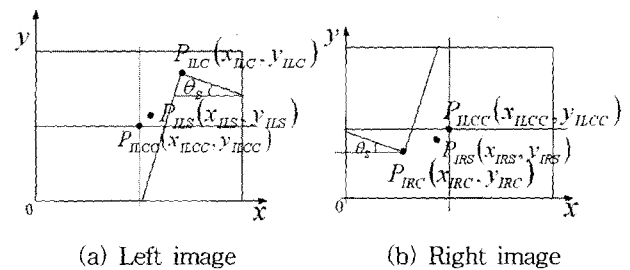


Fig. 11 CCD camera image data with skew angle

Fig. 10 illustrates the situation where the skew angle,  $\theta_s$ , between the spreader and the container exists, while Fig 11 shows the skew angle,  $\theta_s$ , in the CCD camera image.

When there is existence of the skew angle, the height cannot be obtained by using Eq. (6). However note that the sizes of the spreader and the container are equal in the real coordinates. Also we know the corner-points of container in the image coordinates, which are  $P_{ILC}$  and  $P_{IRC}$ , and

corner-points of the spread in the real coordinate, which are  $P_{SLS}$  and  $P_{SRS}$ . Therefore we can assume that the corner coordinates of the spreader are rotated by the amount of the skew angle  $\theta_s$  w.r.t the spreader center point in the real coordinates,  $P_{SSC}$ .

The virtual spreader  $P_{SVLS}(x_{SVLS}, y_{SVLS})$ , which is rotated in the world coordinates for the left corner is defined by

$$\begin{bmatrix} x_{SVLS} \\ y_{SVLS} \end{bmatrix} = \begin{bmatrix} \cos(\theta_s) & -\sin(\theta_s) \\ \sin(\theta_s) & \cos(\theta_s) \end{bmatrix} \begin{bmatrix} x_{SLS} - x_{SSC} \\ y_{SLS} - y_{SSC} \end{bmatrix} + \begin{bmatrix} x_{SSC} \\ y_{SSC} \end{bmatrix} \quad (7)$$

Using the left corner as the world coordinates in Fig. 11, and the x-coordinates for the left corner of spreader by Eq. (7), the height  $d_{sc}$  can be obtained by following equations.

$$x_{IVLS} = x_{ILC} + (d_{lx} - x_{IRC})/2 \quad (8)$$

$$d_{sc} = \frac{(x_{SVLS} - x_{SLCC})d_{lx}}{2(x_{IVLS} - x_{ILCC})\tan\theta_x} \quad (9)$$

#### 4.3 Derivation of the distance error between spreader and container

The image coordinates of the container need to be changed to real coordinate since we need a distance error in the real coordinates instead of in the image coordinates. Eq. (10) changes the image coordinates into the real coordinates.

$$\begin{pmatrix} x_{SLC} \\ y_{SLC} \\ x_{SRC} \\ y_{SRC} \end{pmatrix} = 2d_{sc} \begin{pmatrix} x_{ILC} - x_{ILCC} & 0 \\ 0 & y_{ILC} - y_{ILCC} \\ x_{IRS} - y_{IRCC} & 0 \\ 0 & y_{IRC} - y_{IRCC} \end{pmatrix} \begin{pmatrix} \tan\theta_x \\ d_{lx} \\ \tan\theta_y \\ d_{ly} \end{pmatrix} + \begin{pmatrix} x_{SLCC} \\ y_{SLCC} \\ x_{SRCC} \\ y_{SRCC} \end{pmatrix} \quad (10)$$

Now the container center point in the real coordinate,  $P_{SCC}(x_{SCC}, y_{SCC})$ , becomes

$$x_{SCC} = (x_{SLC} + x_{SRC})/2 \quad (11)$$

$$y_{SCC} = (y_{SLC} + y_{SRC})/2 \quad (12)$$

Therefore, the distance errors of the x-coordinates,  $d_{Ex}$ , and the y-coordinates,  $d_{Ey}$ , can be derived respectively as follows:

$$d_{Ex} = x_{SCC} - x_{SSC} \quad (13)$$

$$d_{Ey} = y_{SCC} - y_{SSC} \quad (14)$$

## 5. Sway information measurement

When the trolley starts to move, it has acceleration, while it has deceleration when it tries to stop. The acceleration and deceleration may cause the spread swings, sway angles, as the result of moment of inertia. To remove out the spread swings, the data of sway angles are to be measured. The conceptual diagram of the sway angle is shown in Fig. 12.  $\theta_{sw}$  represents the sway angle and L represents the wire length which is a major factor for sway period.

### 5.1 Measurement of sway angle by CCD camera

It is necessary to calculate the sway period to obtain the wire length since the sway motion of spreader can be analyzed by means of a pendulum dynamics equation. The spreader is connected to the trolley by four wires with the same lengths. Therefore the sway angle is usually very small.

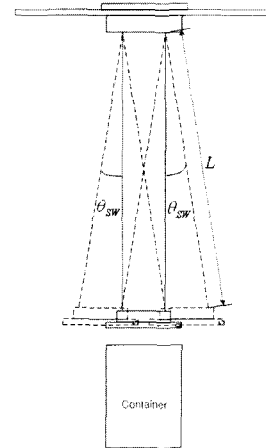


Fig. 12 Conceptual diagram for sway

If the trolley and hoist are stopped, then the sway period of spreader,  $T_{sw}$ , is represented by

$$T_{sw} = 2\pi\sqrt{\frac{L}{g}} \quad (15)$$

where L is the wire length and g is gravitational acceleration. The wire length can be obtained from the lift motor rotary encoder in the trolley.

The distance of the spreader movement is also necessary to calculate the sway angle with the sway period of spreader,  $T_{sw}$ . For that purpose, the corner points of the container are derived from the image data at each sampling instance. The distance of the spreader movement is

obtained by comparing the current corner points of the container with the previous ones. That is, the distance of the spreader movement is calculated at each sampling instance, and Eq. (16) represents the total the distance of the spreader motion.

$$d_s = \sum_{t=0}^{T_{sw}} d_{st} \quad (16)$$

where  $d_{st}$  is the distance of spreader movement at each sampling instance.

The trace of the spreader sway can be approximated as a bisector triangle (refer to Fig. 12), since the sway angle is small. Now the sway angle,  $\theta_{sw}$ , can be calculated by using the data of wire length and the distance of spread movement as follows:

$$\theta_{sw} = \arcsin\left(\frac{d_s / 4}{L}\right) \quad (17)$$

Also the sway acceleration,  $a_{\theta_{sw}}$ , can be defined as

$$a_{\theta_{sw}} = -\frac{g}{L} \sin(\theta) \quad (18)$$

## 6. Experimentation and result

### 6.1 Experiment

The experimental crane for this research is shown in Fig. 13. Its depth and width are 540 mm and 3580 mm, respectively. The crane height is 1640 mm. The experimental container has the size of 240 mm × 600 mm with the height of 130 mm. The laser distance measuring unit is Laser Range Finder LEM<sup>TM3</sup>, the CCD cameras are LG Color CCD Cameras.

The horizontal angle of spreader CCD camera,  $\theta_x$ , is 22.68 degrees, and its vertical image angle,  $\theta_y$ , is 17.95 degree. For the image data, the number of horizontal pixels,  $d_{Ix}$ , is 375, and the number of vertical pixels,  $d_{Iy}$ , is 221. The distance between the CCD camera center point and the corner point of the spreader,  $d_{RS}$ , is 40 mm.

The laser distance measuring unit is placed in the center of the experimental spreader and its working range is from 0.2 to 30 meters with high accuracy, even though it can be used to measure the distance upto 100 meters. During our experiments, the laser distance measuring unit provided the distance to the container with the accuracy of 0.1 mm unless it cannot provide measurements due to environment

obstacles.



Fig. 13 Experimental crane

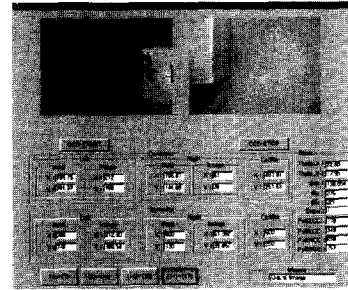


Fig. 14 Experimental program environment

### 6.2 Experiment results

We performed several experiments to verify the proposed algorithms. For the verification of each algorithm, 20 experiments are performed and the results are averaged. As the first experiment, when the spreader has a zero skew angle and real error values are  $d_{Ex}$ : 30 mm  $d_{Ey}$ : 20 mm, and  $d_{sc}$ : 300 mm, an experiment is performed to measure the error. We compared the height data measured by the Laser distance measuring unit and CCD cameras and by only the CCD cameras and the experimental results are shown in Table 1.

As the second experiment, when the spreader has 4 degree skew angles and real values are  $d_{Ex}$ : 30mm  $d_{Ey}$ : 20mm, and  $d_{sc}$ :200mm, a new experiment is performed to measure the error. The measured height by the Laser distance measuring unit with CCD camera and by only the CCD cameras are compared and shown in Table 2.

In measuring skew angles, existence of the laser distance measuring unit does not make any difference since the skew angle measurement is obtained from CCD camera image data. That is, the height,  $d_{sc}$ , between the spreader and the container is not related to the measurement of the skew angle.

Table 1 The first experimental results (Unit : mm)

	$d_{sc}$	$d_{Ex}$	$d_{Ey}$
Real Value	300	30	20
With laser distance measuring unit	300.2	31.2	20.6
Without laser distance measuring unit	295.3	33.7	19.2

Table 2 The second experiment results (Unit : mm)

	$\theta_s$ (degree)	$d_{sc}$	$d_{Ex}$	$d_{Ey}$
Real Value	4	200	30	20
With laser distance measuring unit	4.2	200.1	30.6	20.4
Without laser distance measuring unit	4.2	198.4	28.6	21.1

Table 3 The sway angle measurements (Unit : degree)

	$\theta_{sw}$	$\theta_{sw}$
Real Value	2	3
Measurement Value	1.4	2.1

For the sway angle measurement, the wire length is kept as 1200mm and the test sway angle was 2 degrees for the first measurement and it was 3 degrees for the second. The experimental results are shown in Table 3.

As it is shown in the table, the measurement of sway angles is not accurate since the influence of the disturbances is not considered in this algorithm. Therefore the sway measurement algorithm will be improved later in this paper.

### 5.3 Comparison to other method

In the conventional method for docking where six laser distance measuring units are utilized to match the spreader to the container as shown in Fig. 15.

For the classification of the docking status, it is defined as "ON" for a laser sensor which has the measuring distance value over the standard; it is defined as "OFF" when the distance is shorter than the standard.

Fig. 16 (a) shows the case that all of laser distance measuring units are "ON". Therefore the spreader can land on the container at the moment. In the Fig. 16 (b), right two laser distance measuring units are "OFF". In this case, the spreader has y-axis misalignment error. Therefore the spreader has to be moved to the right for docking. However this algorithm cannot provide the distance value for compensation. While the spreader is moving left and right, the laser distance measuring units may check the status of

each sensor for docking. When all of laser distance measuring units become "ON" like Fig. 16 (a), the spreader may be stopped for docking. So this conventional algorithm cannot control the spreader acceleration for the anti-sway. Fig 16 (c) shows the case that the spreader has the skew angle error which may result the y-axis error as well as the x-axis error. Fig. 17 illustrates the spread arrangement algorithm of the conventional method.

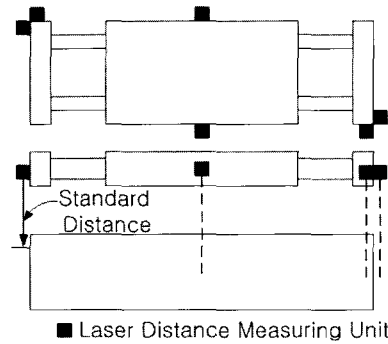


Fig. 15 Docking system with only laser distance measuring units

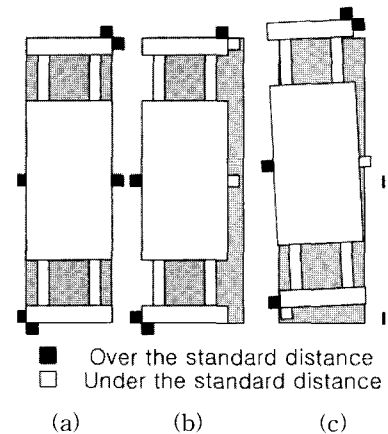


Fig. 16 Classification of the spreader arrangement state

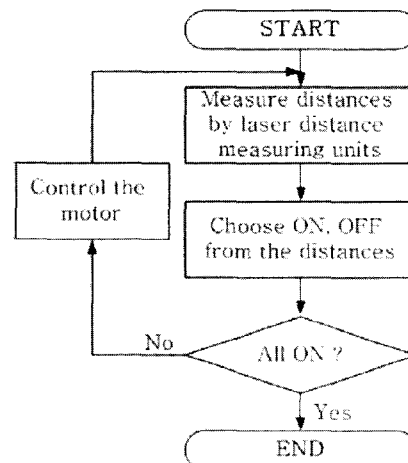


Fig. 17 Experimental flow chart using 6 laser sensors

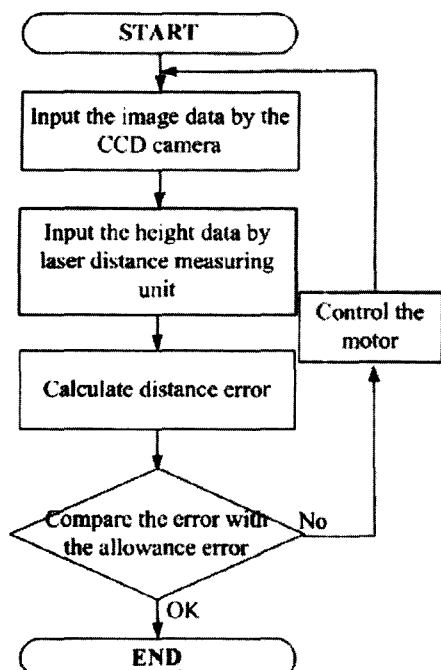


Fig. 18 Experimental flow chart using CCD cameras and laser distance measuring unit

Table 4 Comparison of the measuring performance

	Sway Angle	Precision
The conventional method	1.85°	0.9mm
The proposed method	0.2°	1.1mm

To show the superiority of the proposed algorithm, we performed the same two experiments with the conventional algorithm (Fig. 17) and the new algorithm (Fig. 18) measuring the sway angle and the distance when the crane wire is 1500 mm and the y-axis distance error is 50 mm. The experimental flow for the proposed algorithm is shown in Fig. 18. Table 4 shows the experimental results.

As it is shown in the table 4, the proposed method provides a high sway angle, while it has 0.2 mm larger height error. However the height error is not critical for the docking, while the sway angle should be accurate. If more of laser sensor are installed along the spreader, the sway angle measurement becomes possibly high. However the system becomes too expensive to be applied for the port automation. Therefore the proposed method which utilizes cheap CCD cameras becomes essential as well as economical with the development small CCD cameras.

### 7. Conclusion

This paper demonstrates a new algorithm for deriving the

3D movement information between a spreader and a container of the ALS in automated port system. The edge lines of the container are found by the image pre-processing from the image data of the CCD cameras. It is experimentally recognized that the image preprocessing is very important for the precise measurement of the sway angle as well as the distance. The data of 3D movement and sway information for a yard crane spreader can be used to control ALS (Automatic Landing System) and to decrease accident possibilities for the beginner operator. This algorithm does not exactly reflect the distance information of 3D movement since the image data was scaled-down to improve processing speed. However, with the recent development of computer speed, the original image data can be utilized to measure the 3D movement and sway information, which will verify the superiority of this research further.

### Acknowledgments

This work partially supported by the KOSEF through the CIIPMS at Dong A University.

### References

- [1] Choi, S. U., Lee, J. W., Lee, C. H., Lee, Y. J. and Lee, K. S. (2002), "A development of ATCS for automatic transfer crane", ISIE 2002, Proceedings of the 2002 IEEE International Symposium on, Vol.2, pp.8-11.
- [2] Choi, S. Y., Jin, T. S. and Lee, J. M. (2003), "Optimal Moving Windows for Real-Time Road Image Processing", Journal of Robotics Systems, Vol.20, Issue.2, pp.65-77.
- [3] Duda, R. O. and Hart, P. E. (1972), "Use of hough transform to detect lines and curves in picture", Commun. ACM 15, No.1, pp.11-15.
- [4] David, J. and Kreigman (1986), "Stereo vision and navigation in building for mobile robots", IEEE Trans. On Robotics and Automation, Vol.Ra-2, pp.14-23.
- [5] Gutierrez, M. and Soto, R. (1998), "Fuzzy control of a scale prototype overhead crane", Proc. Of IEEE Conf. on Decision & control, pp.4266-4268.
- [6] Korea Institute of Machinery (2001), "Development of Design and Control Technology For Automated Transfer Crane", Third year report.
- [7] Liu, C. I. and Ioannou, P. A (2002), "A comparison of different AGV dispatching rules in an automated



- container terminal”, Intelligent Transportation Systems, The IEEE 5th International Conference, pp.880 -885.
- [8] Murata, I. and Nakajima, M. (1993), “Automatic control system of container crane(in Japanese with English abstract)”, Trans. JSME, Vol.59, No.564, pp.2401-2407.
- [9] Sonka, M. Hlavac, V. and Boyle, R. (1993), “Image Processing, Analysis and Machine Vision”, CHAPMAN & HALL COMPUTING.
- [10] Park, S. M., Lee, B. K., Jin, T. S. and Lee, J. M. (2003), “Absolute Position Estimation for Mobi Robot Navigation in an Indoor Environment”, Proceeding of the Eighth International Symposium on Artificial Life and Robotics, B-Com Plaza, Beppu, Oita, JAPAN, Vol.2, pp.395-398.
- [11] Gonzalez, R. C. and Woods, R. E. (1993), “Digital Image Processing”, Addison Wesley.

---

**Received** 3 April 2004

**Accepted** 20 June 2004